

Transport processes in metal-insulator granular layers

Y. G. Pogorelov,¹ H. G. Silva,² and J. F. Polido³

¹*IFIMUP and IN-Institute of Nanoscience and Nanotechnology, Universidade do Porto, Rua do Campo Alegre 687, 4169-007 Porto, Portugal*

²*Geophysical Centre of Évora and Physics Department, ECT, University of Évora, Rua Romão Ramalho 59, 7002-554 Évora, Portugal*

³*Ecole Polytechnique Fédérale de Lausanne, Station 1, CH-1015 Lausanne, Switzerland*

(Received 22 September 2010; revised manuscript received 23 December 2010; published 15 March 2011)

Tunnel transport processes are considered in a square lattice of metallic nanogranules embedded into insulating host to model tunnel conduction in real metal/insulator granular layers. Based on a simple model with three possible charging states (\pm or 0) of a granule and three kinetic processes (creation or recombination of a \pm pair, and charge transfer) between neighbor granules, the mean-field kinetic theory is developed. It describes the interplay between charging energy and temperature and between the applied electric field and the Coulomb fields by the noncompensated charge density. The resulting charge and current distributions are found to essentially differ in the free area (FA), between the metallic contacts, or in the contact areas (CA) beneath those contacts. Thus, the steady-state dc transport is compatible only with zero charge density and ohmic resistivity in FA, but charge accumulation and nonohmic behavior are *necessary* for conduction over CA. The approximate analytic solutions are obtained for characteristic regimes (low or high charge density) of such conduction. The comparison is done with the measurement data on tunnel transport in related experimental systems.

DOI: [10.1103/PhysRevB.83.115429](https://doi.org/10.1103/PhysRevB.83.115429)

PACS number(s): 73.40.Gk, 73.50.-h, 73.61.-r

I. INTRODUCTION

More than 3 decades have passed since the pioneering studies by Abeles and coworkers^{1,2} that triggered much research in granular thin films. Actually, nanostructured granular films are of a considerable interest for modern technology due to their peculiar physical properties, like giant magnetoresistance,³ Coulomb blockade,^{4,5} or high-density magnetic memory,⁶ properties that are impossible for continuous materials.

However, a number of related physical mechanisms still need better understanding, in particular, transport phenomena in these films are still a great challenge and, at present, various studies address them.⁷⁻⁹ The main reason is that granular systems reveals certain characteristics which cannot be obtained either in the classical conduction regime (in metallic, electrolyte, or gas discharge conduction) or in the hopping regime (in doped semiconductors or in common tunnel junctions). Their specifics are mainly determined by the drastic difference between the characteristic time of an individual tunneling event ($\sim \hbar/\varepsilon_F \sim 10^{-15}$ s) and the interval between such events on the same granule $\sim e/(jd^2) \sim 10^{-3}$ s, at typical current density $j \sim 10^{-3}$ A/cm² and granule diameter $d \sim 5.0$ nm. Other important moments are the sizable Coulomb charging energy $E_c \sim e^2/(\varepsilon_{\text{eff}}d)$ (typically ~ 10 meV) and the fact that the tunneling rates across the layer may be even several orders of magnitude slower than along it.¹⁰ The interplay of all these factors leads to unusual macroscopic effects, including a peculiar slow relaxation of electric charge discovered in experiments on tunnel conduction through granular layers and granular films.^{11,12} The above-indicated specifics can be contrasted with the well-studied processes of tunnel conduction in the variable-range-hopping (VRH) regime.¹³ The latter approach is more adequate for tunneling between atomic localized states, e.g., in doped semiconductors with shallow dopant levels where the hopping range is defined by the effective localization radius and can extend over many periods of crystalline lattice. Then the competition between

many possible hoppings involves the Coulomb energy cost and defines a certain (temperature-dependent) optimum hopping distance and corresponding conductance laws. In contrast, the granular layers in our consideration permit hoppings only of Fermi electrons between closest-neighbor granules, fixing the hopping distance but including the Coulomb energy effects [also by the image charges in contact area (CA) electrodes].

For theoretical description of transport processes in granular layers (and multilayers) we develop an extension of the classical Sheng-Abeles model for a single layer of identical spherical particles located in sites of a simple square lattice, with three possible charging states (\pm or 0) of a granule and three kinetic processes: creation of a \pm pair (the only process included in the original Sheng-Abeles treatment) on neighbor granules, recombination of such a pair, and charge translation from a charged to neighbor neutral granule. Even this rather simple model, neglecting the effects of disorder within a layer and of multilayered structures, reveals a variety of possible kinetic and thermodynamical regimes, well resembling those observed experimentally.

The detailed formulation of the model, its basic parameters, and its mean-field continuum version are given in Sec. II. In Sec. III we calculate the mean values of occupation numbers of each charging state under steady-state conditions, including the simplest equilibrium situation (no applied fields) in the function of temperature. The analysis of current density and the related kinetic equation in the out-of-equilibrium case is developed in Sec. IV, where its simple, ohmic solution is also discussed for the FA part of the system. The most nontrivial regimes are found for the CA part, as described in Sec. V for steady-state conduction with charge accumulation and nonohmic behavior. The general integration scheme for nonlinear differential equations, corresponding to steady states in free areas (FA) and CA, and the particular approximations leading to their analytic solutions are in the Appendix.

II. CHARGING STATES AND KINETIC PROCESSES

We consider a system of identical spherical metallic nanogranelles of diameter d , located in sites of simple square lattice of period a within a layer of thickness $b \sim a$ of insulating host with a dielectric constant ε (Fig. 1).

In the charge-transfer processes, each granule can bear different numbers σ of electrons in excess (or deficit) of the constant number of positive ions and the resulting excess charge σe defines a Coulomb charging energy $\sim \sigma^2 E_c$. At moderate temperatures, $T \lesssim E_c/k_B$, the consideration can be limited only to the ground neutral state $\sigma = 0$ and single-charged states $\sigma = \pm 1$. Actually, for low metal contents (well separated, small grains) and typical granule size $d \sim 3$ nm in a medium with effective dielectric constant $\varepsilon_{\text{eff}} \sim 25$, we estimate $E_c \sim 20$ meV and, since the energy difference between single-charged and double-charged states is already $3E_c$, the relative smallness of tunnel probability to this state is $\sim \exp(-3E_c/k_B T)$ and the effective temperature limitation reads $T \lesssim 3E_c/k_B \sim 660$ K. This assures the adopted single-charge restriction for the whole temperature range up to at least room temperature.

For a three-dimensional (3D) granular array, E_c was defined in the classic article by Sheng and Abeles,¹ under the assumption of a constant ratio between the mean spacing s and granule diameter d , in the form $E_c = e^2 f(s/d)/(\varepsilon d)$, where the dimensionless function $f(z) = 1/(1 + 1/2z)$. Otherwise, the complete dielectric response of 3D insulating host with the dielectric constant ε and metallic particles with the volume fraction $f < 1$ and diverging dielectric constant $\varepsilon_m \rightarrow \infty$ can be characterized by the effective value $\varepsilon_{\text{eff}} = \varepsilon/(1 - f)$.

For the planar lattice of granules, the analogous effective constant can be estimated, summing the energy $e^2/(\varepsilon d)$ of a charged granule at the $\mathbf{n} = 0$ site and the energy of its interaction with electric dipolar moments $\approx (e/\varepsilon_{\text{eff}})(d/2n)^3 \mathbf{n}$, induced by the Coulomb field from this charge (in macroscopic dielectric approximation) on all the granules at the sites $\mathbf{n} = a(n_1, n_2)$:

$$E_c = \frac{e^2}{d} \left[\frac{1}{\varepsilon} - \frac{\alpha}{\varepsilon_{\text{eff}}^2} \left(\frac{d}{a} \right)^4 \right] = \frac{e^2}{\varepsilon_{\text{eff}} d}. \quad (1)$$

Here the constant $\alpha = \frac{\pi}{4} \sum_{n \neq 0} n^{-4} \approx 5.78$, and the resulting $\varepsilon_{\text{eff}} = [\varepsilon + \sqrt{\varepsilon^2 + \varepsilon \alpha (d/a)^4}] / 2 > \varepsilon$. However, Eq. (1) may considerably underestimate the most important screening from nearest-neighbor granules at $d \sim a$, and in what follows we generally characterize the composite of insulating matrix and metallic granules by a certain $\varepsilon_{\text{eff}} = e^2/dE_c \gg \varepsilon$.

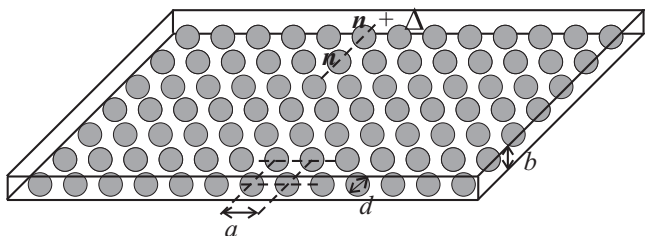


FIG. 1. Square lattice of metallic granules in the insulating matrix.

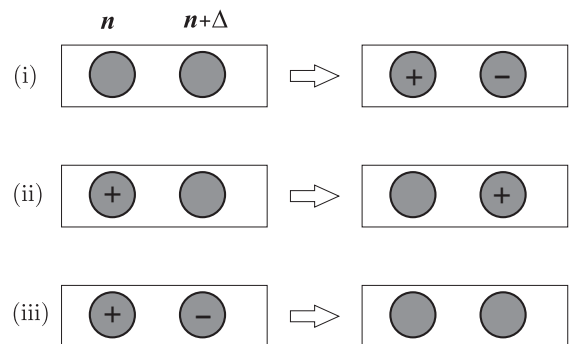


FIG. 2. Kinetic processes in a granular layer.

Following the approach proposed earlier,¹¹ we classify the microscopic states of our system, attributing the charging variable $\sigma_{\mathbf{n}}$ with values ± 1 or 0 to each site \mathbf{n} and then considering three types of kinetic processes between two neighbor granules \mathbf{n} and $\mathbf{n} + \Delta$ (Fig. 2):

(i) *Electron hopping from neutral \mathbf{n} to neutral $\mathbf{n} + \Delta$* , creating a pair of oppositely charged granules: $(\sigma_{\mathbf{n}} = 0, \sigma_{\mathbf{n}+\Delta} = 0) \rightarrow (\sigma_{\mathbf{n}} = +1, \sigma_{\mathbf{n}+\Delta} = -1)$, only this process was included in the Sheng and Abeles's theory;

(ii) *Hopping of an extra electron or hole from \mathbf{n} to neutral $\mathbf{n} + \Delta$* , that is, the charge transfer $(\sigma_{\mathbf{n}} = \pm 1, \sigma_{\mathbf{n}+\Delta} = 0) \rightarrow (\sigma_{\mathbf{n}} = 0, \sigma_{\mathbf{n}+\Delta} = \pm 1)$;

(iii) *Recombination of a electron-hole pair*, the inverse to the process (i): $(\sigma_{\mathbf{n}} = +1, \sigma_{\mathbf{n}+\Delta} = -1) \rightarrow (\sigma_{\mathbf{n}} = 0, \sigma_{\mathbf{n}+\Delta} = 0)$.

Note that all the processes (i) to (iii) conserve the total system charge $Q = \sum_{\mathbf{n}} \sigma_{\mathbf{n}}$, hence, the possibility for charge accumulation or relaxation only appears due to the current leads. A typical configuration for current-in-plane (CIP) tunneling conduction includes two macroscopic metallic electrodes on top of the granular layer, forming CAs where the current is being distributed from the electrodes into granules, through an insulating spacer of thickness b' , and an FA where the current propagates over the distance l between the contacts (Fig. 3). To begin, we consider a simpler case of FA while the specific analysis for CA with an account for screening effects by metallic contacts will be given later in Sec. V.

The respective transition rates $q_{\mathbf{n},\Delta}^{(i)}$ for i th process are determined by the instantaneous charging states of two relevant granules and by the local electric field $\mathbf{F}_{\mathbf{n}}$ and temperature T , accordingly to the expressions:

$$\begin{aligned} q_{\mathbf{n},\Delta}^{(1)} &= (1 - \sigma_{\mathbf{n}}^2) (1 - \sigma_{\mathbf{n}+\Delta}^2) \varphi(e\mathbf{F}_{\mathbf{n}} \cdot \Delta + E_c) \\ q_{\mathbf{n},\Delta}^{(2)} &= \sigma_{\mathbf{n}}^2 (1 - \sigma_{\mathbf{n}+\Delta}^2) \varphi(-e\sigma_{\mathbf{n}} \mathbf{F}_{\mathbf{n}} \cdot \Delta) \\ q_{\mathbf{n},\Delta}^{(3)} &= \frac{1}{2} \sigma_{\mathbf{n}} \sigma_{\mathbf{n}+\Delta} (\sigma_{\mathbf{n}} \sigma_{\mathbf{n}+\Delta} - 1) \varphi(e\sigma_{\mathbf{n}+\Delta} \mathbf{F}_{\mathbf{n}} \cdot \Delta - E_c). \end{aligned} \quad (2)$$

Thus the charging energy is positive, E_c , for the pair creation; zero for the transport; and negative, $-E_c$, for the recombination processes. The function $\varphi(E) = \omega N_F E / [\exp(\beta E) - 1]$ expresses the total probability, at given inverse temperature $\beta = 1/(k_B T)$, for the electron transition between granules with Fermi density of states N_F and Fermi levels differing by E . The hopping frequency $\omega = \omega_a \exp(-2\chi s)$ involves the *attempt frequency*, $\omega_a \sim E_F/\hbar$, the inverse tunneling length χ

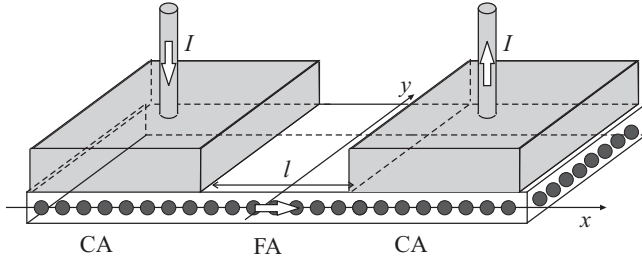


FIG. 3. CIP conduction geometry.

(typically $\sim 10 \text{ nm}^{-1}$), and the intergranule spacing $s = a - d$. Local electric field \mathbf{F}_n on n th site consists of the external applied field \mathbf{A} (site independent) and the Coulomb field \mathbf{C}_n due to all other charges in the system:

$$\mathbf{C}_n = \frac{e}{\epsilon_{\text{eff}}} \sum_{n' \neq n} \sigma_{n'} \frac{\mathbf{n}' - \mathbf{n}}{|\mathbf{n}' - \mathbf{n}|^3}. \quad (3)$$

A suitable approximation is achieved with passing from discrete-valued functions σ_n of discrete argument $\mathbf{n} = a(n_1, n_2)$ to their continuous-valued mean-field (MF) equivalents $\sigma_r = \langle \sigma_n \rangle_r$ (mean charge density) and $\rho_r = \langle \sigma_n^2 \rangle_r$ (mean charge carrier density). These densities are obtained by averaging over a wide-enough area (that is, large compared to the lattice period but small compared to the size of entire system or its parts) around *any* point \mathbf{r} in the plane (for simplicity, we drop the position index at averages $\langle \rangle_r$ in what follows). This also implies passing to a smooth local field:

$$\mathbf{F}_r = \mathbf{A} + \frac{e}{\epsilon_{\text{eff}} a^2} \int \sigma(\mathbf{r}') \frac{\mathbf{r}' - \mathbf{r}}{|\mathbf{r}' - \mathbf{r}|^3} d\mathbf{r}'. \quad (4)$$

and to the averaged transition rates $q_{r,\Delta}^{(i)} = \langle q_{n,\Delta}^{(i)} \rangle$ and $p_{r,\Delta}^{(i)} = \langle \sigma_n q_{n,\Delta}^{(i)} \rangle$. These rates fully define the temporal derivatives of mean densities:

$$\dot{\sigma}_r = \sum_{\Delta} [q_{r,\Delta}^{(1)} - q_{r+\Delta,-\Delta}^{(1)} - p_{r,\Delta}^{(2)} + p_{r+\Delta,-\Delta}^{(2)} - p_{r,\Delta}^{(3)}], \quad (5)$$

$$\dot{\rho}_r = \sum_{\Delta} [q_{r,\Delta}^{(1)} + q_{r+\Delta,-\Delta}^{(1)} - q_{r,\Delta}^{(2)} + q_{r+\Delta,-\Delta}^{(2)} - q_{r,\Delta}^{(3)}]. \quad (6)$$

The set of Eqs. (2)–(6) provides a continuous description of the considered system, once a proper averaging procedure is established.

It can be noted that the issue of multicharged states can be also examined under the effect of an applied field, where E_c needs to be compared with the Coulomb energy change at charge hopping between neighbor granules. Under the most severe conditions when about half of the maximum applied voltage, $\sim 15 \text{ V}$, can drop on the relevant length of few microns in CA (see below in the end of Sec. V), this change will amount to $\sim 25 \text{ meV}$, thus approaching the threshold for multicharge state creation. Nevertheless, such processes can be safely omitted over most of the temperature and voltage regimes in our study.

III. MEAN-FIELD DENSITIES IN EQUILIBRIUM

We perform the above-defined averages in the simplest assumption of no correlations between different sites: $\langle f_n g_{n'} \rangle =$

$\langle f_n \rangle \langle g_{n'} \rangle$, $\mathbf{n}' \neq \mathbf{n}$, and using the evident rules: $\langle \sigma_n^{2k+1} \rangle = \sigma_r$, $\langle \sigma_n^{2k} \rangle = \rho_r$. The resulting averaged rates are

$$\begin{aligned} q_{r,\Delta}^{(1)} &= \sigma_r^0 \sigma_{r+\Delta}^0 \varphi(e\mathbf{F}_r \cdot \Delta + E_c), \\ q_{r,\Delta}^{(2)} &= \sigma_{r+\Delta}^0 [\sigma_r^+ \varphi(-e\mathbf{F}_r \cdot \Delta) + \sigma_r^- \varphi(e\mathbf{F}_r \cdot \Delta)], \\ p_{r,\Delta}^{(2)} &= \sigma_{r+\Delta}^0 [\sigma_r^+ \varphi(-e\mathbf{F}_r \cdot \Delta) - \sigma_r^- \varphi(e\mathbf{F}_r \cdot \Delta)], \\ q_{r,\Delta}^{(3)} &= [\sigma_r^+ \sigma_{r+\Delta}^- \varphi(-e\mathbf{F}_r \cdot \Delta - E_c) \\ &\quad + \sigma_r^- \sigma_{r+\Delta}^+ \varphi(e\mathbf{F}_r \cdot \Delta - E_c)], \\ p_{r,\Delta}^{(3)} &= [\sigma_r^+ \sigma_{r+\Delta}^- \varphi(-e\mathbf{F}_r \cdot \Delta - E_c) \\ &\quad - \sigma_r^- \sigma_{r+\Delta}^+ \varphi(e\mathbf{F}_r \cdot \Delta - E_c)], \end{aligned} \quad (7)$$

where the mean occupation numbers for each charging state $\sigma_r^\pm = (\rho_r \pm \sigma_r)/2$ and $\sigma_r^0 = 1 - \rho_r$ satisfy the normalization condition: $\sum_i \sigma_r^i = 1$.

In a similar way to Eq. (5), we express the vector of average current density \mathbf{j}_n at the n th site:

$$\begin{aligned} \mathbf{j}_n &= \frac{e}{a^2 b} \sum_{\Delta} \Delta [-q_{n,\Delta}^{(1)} + q_{n+\Delta,-\Delta}^{(1)} + p_{n,\Delta}^{(2)} \\ &\quad - p_{n+\Delta,-\Delta}^{(2)} + p_{n,\Delta}^{(3)}], \end{aligned} \quad (8)$$

and then its MF extension \mathbf{j}_r is obtained by simple replacing \mathbf{n} with \mathbf{r} in the arguments of $q^{(i)}$ and $p^{(i)}$. Expanding these continuous functions in powers of $|\Delta| = a$, we conclude that Eq. (5) gets reduced to the usual continuity equation

$$\dot{\sigma}_r = -\frac{a^2 b}{e} \nabla_2 \cdot \mathbf{j}_r, \quad (9)$$

with the two-dimensional (2D) nabla: $\nabla_2 = (\partial_x, \partial_y)$. We begin the analysis of Eqs. (5)–(9) from the simplest situation of a thermal equilibrium in the absence of an electric field, $\mathbf{F}_r \equiv 0$. Equation (5) then turns into $\dot{\sigma}_r \equiv 0$, which indicates zero charge density, and Eq. (8) results in zero current density, $\mathbf{j}_r \equiv 0$, while Eq. (6) provides a finite and constant value of charge carrier density

$$\rho_r \equiv \rho_e = \frac{2}{2 + \exp(\beta E_c/2)}. \quad (10)$$

At low temperatures, $\beta E_c \gg 1$, this value is exponentially small [$\rho_e \approx 2 \exp(-\beta E_c/2)$], and for high temperatures, $\beta E_c \ll 1$, it behaves as $\rho_e \approx \rho_\infty - \beta E_c/9$, tending to the limit $\rho_\infty = 2/3$, which corresponds to equipartition between all three fractions σ^i (Fig. 4, although this limit is beyond the actual validity of the model, as indicated in Sec. II).

In the presence of electric fields $\mathbf{F}_r \neq 0$, the local equilibrium should be perturbed and the system should generate current and generally accumulate charge. Then, from Eq. (6), the charge density σ_r is related to the carrier density ρ_r as

$$\sigma_r^2 = \frac{(\rho_r - \rho_e)(\rho_r + \rho_e - 2\rho_e \rho_r)}{(1 - \rho_e)^2}, \quad (11)$$

describing the increase of charge density with going away from equilibrium. As seen from Fig. 5, for moderate temperatures, $T \lesssim E_c/k_B$, where the neglect of multiple charged states is

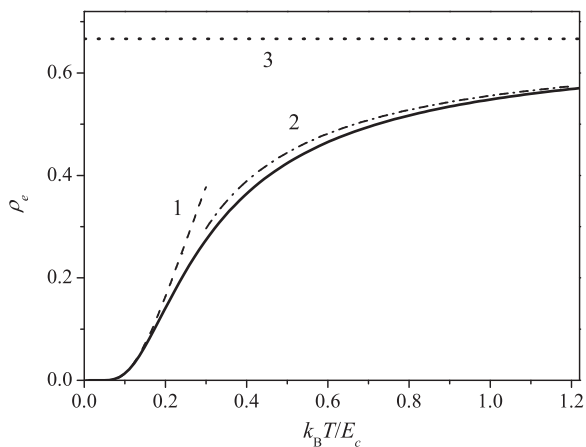


FIG. 4. Equilibrium density ρ_e of charge carriers in the function of temperature (solid line). Curve 1 (dashed line) corresponds to the low-temperature asymptotics $\rho_e \approx 2 \exp(-E_c/2k_B T)$ and curve 2 (dash-dotted line) to the high-temperature asymptotic $\rho_e \approx \rho_\infty - E_c/9k_B T$, converging to the limit $\rho_\infty = 2/3$ (dotted line).

justified, this dependence is reasonably close to the simplest low-temperature form:

$$\sigma \approx \sqrt{\rho^2 - \rho_e^2}, \quad (12)$$

that will be used in what follows.

Now we are in a position to address the out-of-equilibrium situations, beginning with a simpler case of dc current flowing through the FA.

IV. STEADY-STATE CONDUCTION IN FA

In the presence of (generally nonuniform) fields \mathbf{F}_r and densities σ_r, ρ_r , we expand Eq. (8) up to first-order terms in $|\Delta| = a$ and obtain the local current density as a sum of two contributions, the field-driven and diffusive:

$$\mathbf{j}_r = \mathbf{j}_r^{\text{field}} + \mathbf{j}_r^{\text{dif}} = g(\rho_r) \mathbf{F}_r - eD(\rho_r) \nabla_2 \sigma_r, \quad (13)$$

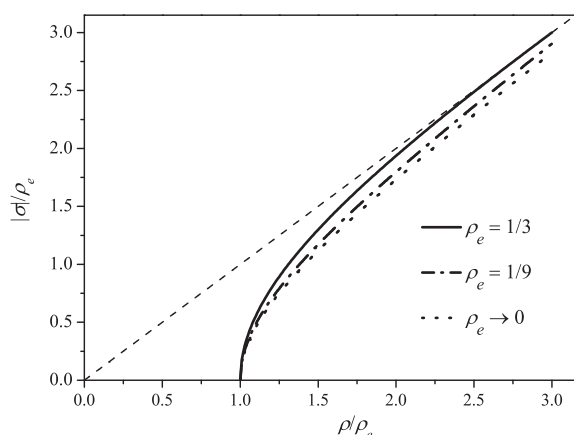


FIG. 5. The charge density σ in function of the carrier density ρ for different temperatures (corresponding to different thermal equilibrium values ρ_e). Note the closeness of all the curves to that for the low-temperature limit $\rho_e \rightarrow 0$, given exactly by Eq. (12).

where the effective conductivity g and diffusion coefficient D are functions of the local charge carrier density, $\rho \equiv \rho_r$:

$$g(\rho) = \frac{e^2}{b} \left| 2(1 - \rho)^2 \varphi'(E_c) + \rho(1 - \rho) \varphi'(0) + \frac{1}{2}(\rho^2 - \sigma^2) \varphi'(-E_c) \right|, \quad (14)$$

$$D(\rho) = \frac{\rho(1 - \rho_e)^2 \varphi(0)(1 - \rho) \rho_e^2 \varphi(-E_c)/2}{\rho(1 - 2\rho_e) + \rho_e^2}.$$

In view of Eqs. (11) and (12), we can consider g and D as even functions of local charge density σ , and only this dependence will be used below. Moreover, g and D depend on temperature through the functions φ and φ' . The system of Eqs. (11)–(14), together with Eq. (4), is closed and self-consistent, defining the distributions of σ_r and ρ_r at given \mathbf{j}_r . It is readily apparent that the trivial solution, $\sigma(x) \equiv 0$, is a valid one and now we argue that in fact this is the only practical solution for FA.

First, we note physical restrictions on the charge accumulation in FA. By the problem symmetry, the charge density should depend only on the coordinate along the current, $\sigma = \sigma(x)$, this function being odd (in the geometry of Fig. 3) and supposedly monotonous. Its maximum value $\sigma_{\text{max}} = \sigma(L/2)$ will then define the characteristic scale for the Coulomb field, $C \sim \sigma_{\text{max}} e / (\epsilon_{\text{eff}} a^2)$, which should not be higher than typical applied fields, $A \sim 10^2$ V/cm (as seen from the relatively moderate nonohmic vs. ohmic response in the experiment). Thus the maximum charge density should not surpass the level of $A \epsilon_{\text{eff}} a^2 / e \sim 10^{-3}$, which is much lower than the equilibrium density of charge carriers ρ_e (except for, maybe, too-low temperatures, $T \lesssim 0.07 E_c / k_B \sim 10$ K). Therefore, one can neglect the small difference, Eq. (12), setting constant values: $\rho \approx \rho_e$ and then $g \approx g_e \equiv g(\rho_e)$ and $D \approx D_e \equiv D(\rho_e)$.

Under such a condition, we can eliminate the (relatively unknown) constant A from Eq. (13), which brings this equation to the following integrodifferential form:

$$\frac{\partial^2 \sigma(x)}{\partial x^2} = \frac{g_e}{D_e \epsilon_{\text{eff}} a^2} P \int_{-1/2}^{1/2} \frac{\sigma(x') dx'}{(x - x')^2}, \quad (15)$$

where the P symbol at integration in x' means the “discrete principal value,” which is omission of the interval $(x - a, x + a)$ to avoid the apparent divergence, in agreement with the minimum distance between granules in the lattice. Thus the regularized integral converges rapidly, so it is reasonable to fix the argument of σ density at $x' = x$, arriving at a simple differential equation:

$$\frac{\partial^2 \sigma(x)}{\partial x^2} = \frac{\sigma(x)}{r_\beta^2}. \quad (16)$$

Here the parameter

$$r_\beta^2 = \frac{a^3}{d} \frac{2e^{\beta E_c} + 5e^{\beta E_c/2} + 2}{e^{3\beta E_c/2} + 2\beta E_c e^{\beta E_c} - e^{\beta E_c/2}}$$

defines the temperature-dependent length scale r_β , and the x -odd solution of Eq. (16) is just $\sigma(x) = \sigma_1 \sinh(x/r_\beta)$. However, for all the considered temperatures, $\beta E_c \gtrsim 1$ (see the note in Sec. II), this scale is $r_\beta \lesssim a$, that is by many orders of magnitude smaller than the FA size l . Then the estimate for

the constant σ_1 in the above solution, $\sigma_1 \sim \sigma_{\max} e^{-l/r_\beta}$ with the exponent as great as, for instance, $l/r_\beta \sim 10^4$, makes this solution practically vanishing within whole FA, except maybe for a very narrow vicinity $\sim r_\beta$ of its interface with CA [where, strictly speaking, Eq. (16) no more holds]. This evident consequence of long-range character of Coulomb fields in FA will be contrasted below with the situation in CA, where charge accumulation becomes possible due to screening effects by the metallic contacts and to the related short-range fields.

Thus we conclude that there is practically no charge accumulation and hence no diffusive contribution to the current in FA. Thus the steady state of FA in out-of-equilibrium conditions should be characterized by the ohmic conductivity g_e . In fact, an estimation (based on an experimental system¹⁵) suggests that the FA contribution to the overall resistance turns out to be about two orders of magnitude smaller than the CA one (see below), and thus the transport is expected to be mainly controlled by CA.

V. STEADY-STATE CONDUCTION IN CA

The kinetics in CA includes, in addition to the processes (i)–(iii) of Secs. III and IV, four additional microscopic processes between the n th granule and the electrode (Fig. 6) which are responsible for variations of total charge Q by ± 1 . The respective rates $q^{(i)}$, $i = 4, \dots, 7$, are also dependent on the charging state (σ_r, ρ_r) of the relevant granule and, using the same techniques as before, their mean values are

$$\begin{aligned} q_r^{(4)} &= (\rho_r + \sigma_r)\psi(-U - E'_c), & q_r^{(5)} &= (\rho_r - \sigma_r)\psi(U - E'_c), \\ q_r^{(6)} &= (1 - \rho_r)\psi(U + E'_c), & q_r^{(7)} &= (1 - \rho_r)\psi(-U + E'_c). \end{aligned} \quad (17)$$

Here the function $\psi(E)$ formally differs from $\varphi(E)$ only by changing the prefactor: $\omega \rightarrow \omega' = \omega_a e^{-2\chi b'} \ll \omega$, but the arguments of these functions in Eq. (17) include other characteristic energies. Thus, the energy $U = eb'S$ is due to the electric field $S \equiv F_c(z = b')$ at the contact surface above the granule. As seen from Fig. 7, this field is always normal to the surface and its value is defined by the local charge density σ (see below). At least the charging energy E'_c for a granule under the contact can be somewhat lower (e.g., by $\sim 1/2$) than E_c . Then the kinetic equations in interface region present a

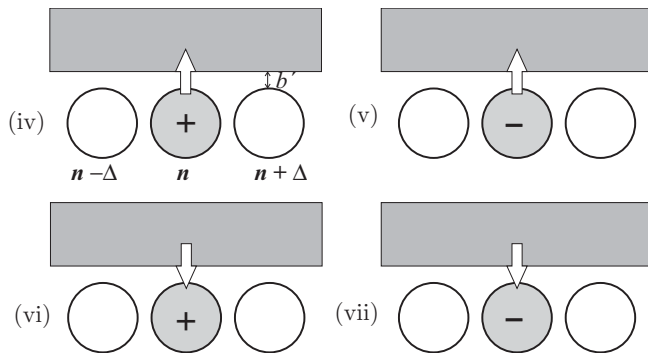


FIG. 6. Kinetic processes between n th granule and the metallic electrode in CA.

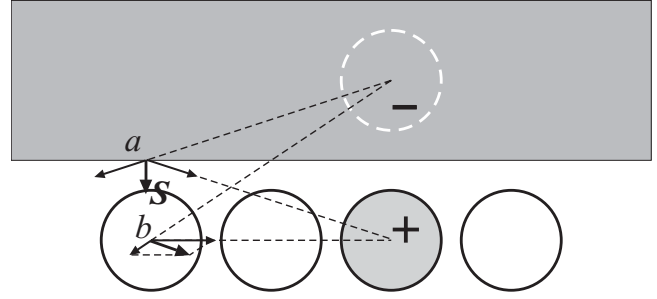


FIG. 7. Formation of local electrical fields by a dipole of a charged granule and its (oppositely charged) image: at the surface of the metallic electrode (point a) and on other granule (point b).

generalization of Eqs. (5)–(6), as follows:

$$\begin{aligned} \dot{\sigma}_r &= \sum_{\Delta} [q_{r,\Delta}^{(1)} - q_{r+\Delta,-\Delta}^{(1)} - p_{r,\Delta}^{(2)} + p_{r+\Delta,-\Delta}^{(2)} - p_{r,\Delta}^{(3)} \\ &\quad - q_r^{(4)} + q_r^{(5)} + q_r^{(6)} - q_r^{(7)}], \end{aligned} \quad (18)$$

$$\begin{aligned} \dot{\rho}_r &= \sum_{\Delta} [q_{r,\Delta}^{(1)} + q_{r+\Delta,-\Delta}^{(1)} - q_{r,\Delta}^{(2)} + q_{r+\Delta,-\Delta}^{(2)} - q_{r,\Delta}^{(3)} \\ &\quad - q_r^{(4)} - q_r^{(5)} + q_r^{(6)} + q_r^{(7)}]. \end{aligned} \quad (19)$$

The additional terms, by the *normal* processes (iv)–(vii), are responsible for appearance of a *normal* component of current density:

$$j_r^z = \frac{e}{a^2} [q_r^{(4)} - q_r^{(5)} - q_r^{(6)} + q_r^{(7)}], \quad (20)$$

in addition to the planar component, still given by Eq. (8). But an even more important difference from the FA case is the fact that the Coulomb field here is formed by a *double layer* of charges, those by granules themselves and by their images in the metallic electrode (Fig. 7). Summing the contributions from all the charged granules and their images (except for the image of n th granule itself, already included in the energy E'_c), we find that the above-mentioned field at the contact surface above the point \mathbf{r} of the granular layer, S_r , can be expressed as a *local* function of the charge density σ_r :

$$S_r = C_r(z = b') = -\frac{4\pi e}{\varepsilon a^2} \sigma_r, \quad (21)$$

replacing the integral relations, Eqs. (3)–(4), in FA. Also, note that the relevant dielectric constant for this field formed outside the granular layer is rather the host value ε than the renormalized ε_{eff} within the layer [as by Eq. (3)]. The planar component of the field by charged granules $\mathbf{F}_r^{\text{pl}} = \mathbf{C}_r(z = 0)$ is then determined by the above-defined normal field S_r through the relation $\mathbf{F}_r^{\text{pl}} = b' \nabla_2 S_r$. The density of planar current is $\mathbf{j}_r^{\text{pl}} = g \mathbf{F}_r^{\text{pl}} - e D \nabla_2 \sigma_r$, according to Eq. (13), that is, both field-driven and diffusive contributions into \mathbf{j}_r^{pl} are present here and both are proportional to the gradient of σ_r . In the low-temperature limit, this proportionality is given by

$$\mathbf{j}_r^{\text{pl}} \approx - \left[\frac{8\pi e^3 \omega N_F b'}{\varepsilon_{\text{eff}} a^3} g(\sigma_r) + \frac{e \omega N_F k_B T}{a} \right] \nabla_2 \sigma_r. \quad (22)$$

Note that the presence of a nonlinear function

$$g(\sigma) = \sqrt{\rho_e^2 + \sigma^2} - 2\rho_e^2 - \sigma^2,$$

defines a *nonohmic* conduction in CA. In fact, this function should be defined by Eq. (21) only for charge density below its maximum possible value $|\sigma_{\max}| = \sqrt{1 - \rho_e^2}$, turning zero for $|\sigma| > |\sigma_{\max}|$ (note that the latter restriction just corresponds to our initial limitation to the single-charged states; see Sec. II). In the same limit of low temperatures, the normal current density is obtained from Eqs. (16) and (17) as $\mathbf{j}_z(\mathbf{r}) = G_z \Sigma_{\mathbf{r}}$, where $G_z \approx \omega' N_F E'_c \varepsilon_{\text{eff}} / 4\pi$. Finally, the kinetic equation in this case is obtained, in analogy with Eq. (8), as

$$\dot{\sigma}_{\mathbf{r}} = -\frac{a^2 b}{e} \nabla_2 \cdot \mathbf{j}_{\mathbf{r}}^{\text{pl}} + \frac{a^2}{e} j_{\mathbf{r}}^z. \quad (23)$$

This equation permits us to describe the steady-state conduction as well as various time-dependent processes. The first important conclusion is that steady-state conduction in the interface becomes possible only at the nonzero charge-density gradient, that is, *necessarily* involving charge accumulation, in contrast to the above-considered situation in total.

Let us restrict the analysis to the steady-state conduction regime which is simpler, though the obtained results can be used also for the analysis of a more involved case when an explicit temporal dependence of charge density is included in Eq. (23) (this will be a topic of future study).

We choose the contacts geometry in the form of a rectangular stripe of planar dimensions $L \times L'$, along and across the current, respectively. Ignoring relatively small effects of current nonuniformity along the lateral boundaries, the only relevant coordinate for the problem is longitudinal, x (Fig. 8), so we consider the relevant function σ_x with its derivatives, spatial σ'_x and temporal $\dot{\sigma}_x$. In the steady-state regime, $\dot{\sigma} = 0$ in Eq. (23), and the total current $I = \text{const}$, defined by the action of external source. Using the above approximation for $g(\sigma)$, a nonlinear second-order equation for charge density is then found:

$$\frac{d}{dx} \{ [g(\sigma_x) + \tau] \sigma'_x \} - k^2 \sigma_x = 0. \quad (24)$$

Here the parameters are $k^2 = (\omega' E'_c) / (ab\omega k_B T_1)$ and $\tau = T/T_1$, where T is the actual temperature and $T_1 = 8\pi e^2 b' / a^2 k_B \varepsilon_{\text{eff}}$. To define completely its solution, the following boundary conditions are imposed:

$$\sigma'_{x=0} = \frac{k^2 b' \sigma_{x=0}}{g(\sigma_{x=0}) + \tau}, \quad (25)$$

$$\sigma'_{x=L} = \frac{a}{Le\omega b N_F k_B T_1} \frac{I}{g(\sigma_{x=L}) + \tau}. \quad (26)$$

Here Eq. (25) corresponds to the fact that the longitudinal current j^x at the initial point of the contact-granular sample interface (the leftmost arrow in Fig. 8) is fully supplied by the normal current j^z entering from the contact to the granular sample, and Eq. (26) corresponds to the current continuity at passage from CA (of length L along the x axis) to FA.

Let us discuss the solution of Eq. (24) qualitatively. Generally, to fulfill the conditions, Eqs. (25) and (26), one needs a quite subtle balance to be maintained between the charge density and its derivatives at both ends of contact

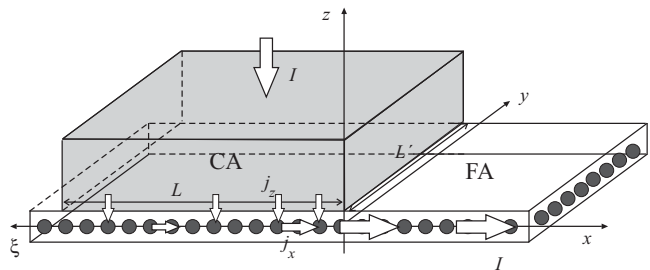


FIG. 8. Relations between longitudinal (j_x) and normal (j_z) currents in CA, adding to the total current I .

interface. But the situation is radically simplified when the length L is much greater than the characteristic decay length for charge and current density: $kL \gg 1$. In this case, the relevant coordinate is $\xi = L - x$, so the boundary condition (25) corresponds to $\xi = L \rightarrow \infty$, when both its left- and right-hand side turn zeros:

$$\sigma_{\xi \rightarrow \infty} = 0, \quad \sigma'_{\xi \rightarrow \infty} = 0. \quad (27)$$

The numeric solution shows that, for any initial [with respect to ξ , which is related to $x = L$, Eq. (26)] value of charge density $\sigma_{\xi=0} = \sigma_0$, there is a *unique* initial value of its derivative $\sigma'_{\xi=0} = D(\sigma_0)$ which just assures the limits, Eq. (27), while for $\sigma'_{\xi=0} > D(\sigma_0)$ the asymptotic value diverges as $\sigma_{\xi \rightarrow \infty} \rightarrow \infty$, and for $\sigma'_{\xi=0} < D(\sigma_0)$ it diverges as $\sigma_{\xi \rightarrow \infty} \rightarrow -\infty$. Then, using the boundary condition, Eq. (26), and taking into account the relation $V = V_0 \sigma_0$ following from Eq. (23) with $V_0 = 4\pi e b' / (\varepsilon_{\text{eff}} a^2)$, we conclude that the function $D(\sigma_0)$ generates the I - V characteristics:

$$I = I_1 b' D\left(\frac{V}{V_0}\right) \left[g\left(\frac{V}{V_0}\right) + \tau \right], \quad (28)$$

where $I_1 = e\omega N_F k_B T_1$.

A more detailed analysis of Eq. (24) is presented in the Appendix. In particular, for the weak current regime (Regime I) when $\sigma_0 \ll \sigma_1 = \sqrt{32\rho_e(\rho_e + \tau)} \ll 1$, so $g(\sigma) \approx \rho_e + \sigma^2 / (2\rho_e)$ along whole the contact interfaces, Eq. (23) admits an approximate analytic solution:

$$\sigma_{\xi} = \sigma_0 e^{-\lambda \xi} \left[1 + 6 \left(\frac{\sigma_0}{\sigma_1} \right)^2 (1 - e^{-2\lambda \xi}) \right], \quad (29)$$

with the exponential decay index $\lambda = k / \sqrt{\rho_e + \tau}$.

This results in the explicit I - V characteristics for Regime I:

$$I = G_0 V \left[1 + \left(\frac{V}{V_1} \right)^2 \right], \quad (30)$$

for $V < V_1 = \sigma_1 V_0$, Eq. (30) describes the initial ohmic CA conductance (temperature τ dependent):

$$G_0 = \frac{I_1 k b'}{V_0} \sqrt{\rho_e(\tau) + \tau}. \quad (31)$$

It is of interest to note the difference between the low-temperature behavior $\sim T^{1/2}$ of Eq. (31) and typical VRH behavior by the $\sim \exp[-(T_0/T)^{1/4}]$ Mott law.¹³ The voltage dependence here becomes nonohmic for $V \sim V_1$. But at so high voltages another conduction regime already applies (called

Regime II), where $\sigma_1 \ll \sigma_0 \ll 1$ and one has $g(\sigma) \approx \sigma$ [see Eq. (21)]. Following the same reasoning as for the Regime I, we obtain a nonlinear I - V characteristics for Regime II:

$$I \approx \frac{I_1 k b'}{\sqrt{3 V_0^3}} (V + V_0 \tau)^{3/2} \quad (32)$$

and this law is less temperature dependent than Eq. (30), which is related to the fact that the conductance in Regime II is mainly due to dynamical accumulation of charge and not to thermic excitation of charge carriers. Interestingly a $I \propto V^{3/2}$ law was recently found in experimental measurements.¹⁵ Further, such nonlinearity can be yet more pronounced if multiple charging states are engaged, as may be the case in real granular layers with a certain statistical distribution of granule sizes present.

At least, for even stronger currents, when already $\sigma_0 \sim 1$, the solutions of Eq. (24) can be obtained numerically, following the above discussed procedure of adjustment of the derivative $D(\sigma_0)$ to a given σ_0 . Such solutions have an asymptotic behavior of the following type: $I \propto V^{5/4}$.

A simple and important exact relation for the total accumulated charge Q in CA is obtained from the direct integration of Eq. (24):

$$Q = tI,$$

where the parameter $t = 1/\psi(-E'_c)$ should have a role of characteristic relaxation time in nonstationary processes. Assuming its value $t \sim 1$ s (comparable with the experimental observations¹¹), together with the above used values of ω and T_1 , we conclude that the characteristic length scale λ^{-1} for solutions of Eq. (24) can reach up to $\sim 10^3 a \sim 1 \mu\text{m}$, which is a reasonable scale for a charge distribution beneath the contacts.

VI. GLOBAL CONDUCTION IN THE SYSTEM

The conduction in the overall system results from matching the above-considered processes in CA and FA. Thus, in order to evaluate the global resistance of this circuit in series it is necessary to add the contributions of both areas to it. Recent measurements¹⁵ have shown notably nonlinear I - V curves (already at low-enough voltages), so, accordingly with the above discussion, this indicates that the resistance should be dominated by CA. To have a clear view on it, we can use the typical parameters for the granular film ($a \sim 5$ nm, $d \sim 4$ nm, $\chi \sim 10$ nm⁻¹, $b \sim 8$ nm, $b' \sim 2$ nm, $E_c \sim 10$ meV, $N_F \sim 1$ eV⁻¹) and take ω as a (less-known) fitting parameter. For the considered rectangular CIP geometry we also use the experimental values¹⁵ of width $L' = 3$ mm and of distance between the contacts $l = 100 \mu\text{m}$.

Choosing $T = 50$ K, the ohmic conductance of the FA, G_{FA} , can be calculated through the formula $G_{\text{FA}} = g(\rho_e)L'b/l \approx \omega 1.5 \times 10^{-18}$ S. In the CA, we can estimate the conductance (in Regime I) following the above formula $G_{\text{CA}} \approx \omega 8.0 \times 10^{-22}$ S. Thus it is clear that, for any choice of ω , the conductance of the CA is about 4 orders of magnitude smaller than that of the FA and for that reason it should dominate the global resistance of the system. Then, using the formulas, Eqs. (29)–(31), we obtain a good agreement with the experimental data by Ref. 15 as shown in Fig. 9. It should be noted,

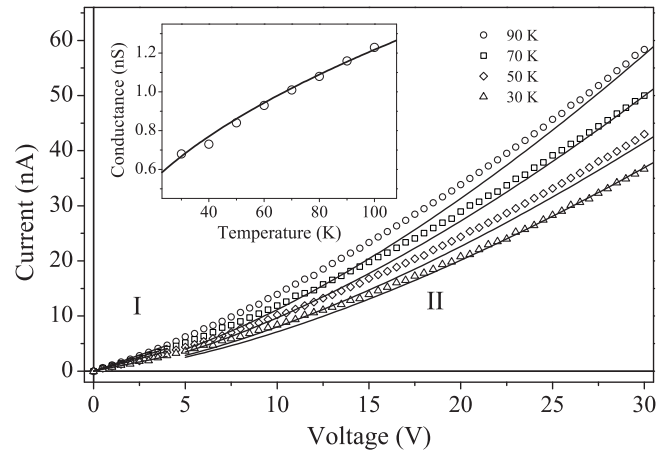


FIG. 9. I - V characteristics for a granular sample at different temperatures, compared with the theoretical curves for Regimes I and II. (Inset) Temperature dependence of ohmic conductance G_0 , measured data (circles) vs. calculated by Eq. (31).

however, that the effective value of the parameter V_0 giving the best fit to the experimental data should be notably higher than that given by our formula [before Eq. (28)] for a single-layer system. Thus, with the above choice of other parameters, we have the single-layer value $V_0 \approx 0.5$ V, whereas the best fit for the 10-layer experimental sample needs instead $V_{\text{exp}} \approx 3$ V. This difference can be effectively accounted for by a simple multiplicative factor $\alpha \approx 6$ (the “multilayer factor”) so $V_{\text{exp}} = \alpha V_0$ assures both the agreement for Regimes I and II of I - V curves and the boundary $V \sim V_{\text{exp}}$ between them, clearly shown in Fig. 9.

The obtained results can be also compared with the well-known work by Kulik and Shekhter on tunnel conduction through granular media.¹⁶ They considered the classical situation of tunnel junction, which is commonly referred to in spintronics as current-perpendicular-to-plane geometry. There the model can be only restricted to charge transfers between a granule and metallic electrodes. Also such geometry allows to excite multicharged granule states by the applied field effect (much stronger in that case than in ours), producing characteristic spikes in the conductance vs. voltage. Our approach considers an opposite case of CIP geometry, where charge creation and recombination processes are included in addition to charge transfers and the effects of space charge by granules are more pronounced, producing the crossover from ohmic to nonohmic conductance vs. voltage. The difference between the two regimes is seen by comparing of Figs. 3 and 4 in Ref. 16 and our Fig. 9.

VII. CONCLUSION

In conclusion, the mean-field model is developed for tunnel conduction in a granular layer, including three principal processes of creation and annihilation of pairs of opposite charges on neighbor granules and of charge transfer from a charged granule to a neighbor neutral granule. Effective kinetic equations for averaged charge densities are derived for the characteristic areas of the granular sample: the contact areas beneath metallic current leads and free area between these

leads. From these kinetic equations, it is shown that the tunnel conduction in the free area does not produce any notable charge accumulation, and the conduction regime here is purely ohmic. Contrariwise, such conduction in the contact area becomes impossible without charge accumulation, leading to a generally nonohmic conduction regime, since the contact area dominates in the overall resistance. Approximate analytic treatment is developed for calculation of charge density and tunnel current in two characteristic regimes: (I) for weak charge accumulation (compared to the thermal density of charge carriers) and (II) for strong charge accumulation, leading to a non-ohmic $I \propto V^{3/2}$ conduction law. The calculated I - V curves and temperature dependencies are found in a good agreement with available experimental data. The proposed model can be further developed for description of multilayer structure effects and also of non-stationary conduction processes, like anomalous slow current relaxation.¹⁷ Finally, the elastic effects of Coulomb forces by charged granules can be included in order to explain the remarkable phenomenon of resistive-capacitive switching,¹⁸ in granular layered conductors.

ACKNOWLEDGEMENTS

The authors are grateful to G. N. Kakazei, J. A. M. Santos, J. B. Sousa, J. P. Araújo, J. M. B. Lopes dos Santos, and H. L. Gomes for kind assistance and valuable help in various parts of this work. One of us (H.G.S.) gratefully acknowledges the support from Portuguese FCT through Grant No. SFRH/BPD/63880/2009.

APPENDIX

Let us consider the equation:

$$\frac{d}{d\xi} [g(\sigma) + \tau] \frac{d\sigma}{d\xi} - k^2\sigma = 0 \quad (\text{A1})$$

with certain boundary conditions $\sigma(0) = \sigma_0$, $\sigma'(0) = \sigma'_0$, resulting from Eqs. (24) and (25). For a rather general function $g(\sigma)$ we can define the function

$$f(\sigma) = \int_0^\sigma g(\sigma') d\sigma'. \quad (\text{A2})$$

Equation (A1) presents itself as:

$$\frac{d^2 F_\xi}{d\xi^2} = k^2 \sigma_\xi, \quad (\text{A3})$$

where $F_\xi \equiv f(\sigma_\xi) + \tau\sigma_\xi$. Considered irrespectively of ξ :

$$f(\sigma) + \tau\sigma = F, \quad (\text{A4})$$

this equation also defines σ as a certain function of F : $\sigma = \sigma(F)$. Hence it is possible to construct the following function:

$$\phi(F) = 2 \int_0^F \sigma(F') dF'. \quad (\text{A5})$$

Now, multiplying Eq. (A3) by $2dF/d\xi$, we arrive at the equation:

$$\frac{d}{d\xi} \left(\frac{dF}{d\xi} \right)^2 = k^2 \frac{d\phi}{d\xi}, \quad (\text{A6})$$

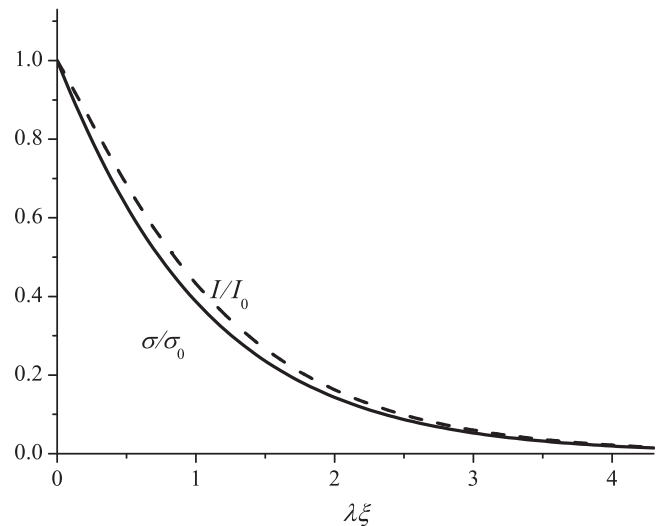


FIG. 10. Charge density and current distribution in the CA region (Regime I).

with $\phi(\xi) \equiv \phi(F_\xi)$. Integrating Eq. (A6) in ξ , we obtain a first-order separable equation for F_ξ :

$$\frac{dF}{d\xi} = \pm k \sqrt{\phi(F)}. \quad (\text{A7})$$

We expect the function F to decrease at going from $\xi = 0$ into depth of interface region, hence choose the negative sign on right-hand side of Eq. (A7) and obtain its explicit solution as

$$\int_{F_\xi}^{F_0} \frac{dF'}{\sqrt{\phi(F')}} = k\xi \quad (\text{A8})$$

with $F_0 = f(\sigma_0) + \tau\sigma_0$. Finally, the sought solution for $\sigma_\xi = \sigma(F_\xi)$ results from substitution of the function F_ξ , given implicitly by Eq. (A8), into $\sigma(F)$ defined by Eq. (A4). Consider some particular realizations of the above scheme.

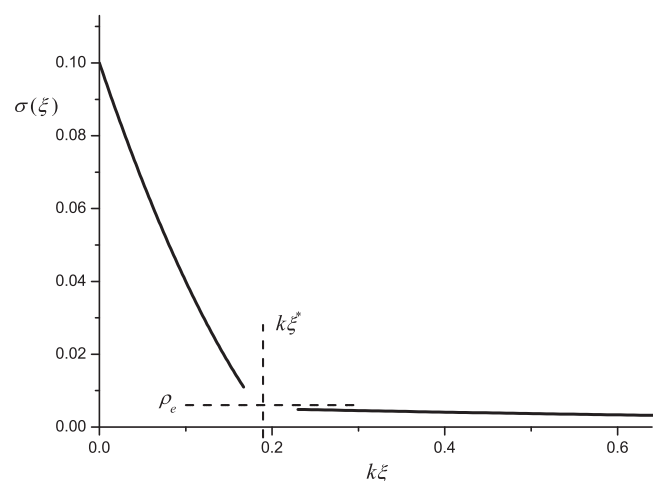


FIG. 11. Charge density distribution in Regime II. A fast decay is changed to a slower exponential law, after density dropping below the characteristic value ρ_e .

For the approximate solution of $g(\sigma)$ given above, we have the explicit integral, Eq. (A2), in the form:

$$F(\sigma) = f(\sigma) + \tau\sigma = \left(\tau + \frac{\sqrt{\rho_e^2 + \sigma^2}}{2} - \rho_0^2 - \frac{\sigma^2}{3} \right) \sigma + \rho_e^2 \ln \sqrt{\frac{\sigma + \sqrt{\rho_e^2 + \sigma^2}}{\rho_e}}. \quad (\text{A9})$$

In the case $\sigma \ll \rho_e \ll 1$ (Regime I), Eq. (A9) is approximated as:

$$F \approx (\rho_e + \tau)\sigma + \frac{\sigma^3}{6\rho_e}, \quad (\text{A10})$$

hence $\sigma(F)$ corresponds to a real root of the cubic equation, Eq. (A10), and in the same approximation of Regime I it is given by:

$$\sigma(F) \approx \frac{F}{\rho_e + \tau} \left(1 - \frac{8F^2}{\sigma_1^2} \right), \quad (\text{A11})$$

with $\sigma_1 = 4\sqrt{\rho_e(\rho_e + \tau)^3}$. Using this form in Eq. (A5), we obtain:

$$\varphi(F) \approx \frac{F^2}{\rho_e + \tau} \left(1 - \frac{4F^2}{\sigma_1^2} \right), \quad (\text{A12})$$

and then substituting into Eq. (A8):

$$\ln \frac{[1 + \sqrt{1 - (2F/\sigma_1)^2}]F_0}{[1 + \sqrt{1 - (2F_0/\sigma_1)^2}]F} = \lambda\xi. \quad (\text{A13})$$

Inverting this relation, we define an explicit solution for F_ξ :

$$F(\xi) \approx F_0 e^{-\lambda\xi} \left[1 + \frac{F_0^2}{\sigma_1^2} (1 - e^{-2\lambda\xi}) \right]. \quad (\text{A14})$$

Finally, substituting Eq. (A14) into Eq. (A11), we arrive at the result of Eq. (29) corresponding to Fig. 10.

For the Regime II we have in a similar way:

$$F(\sigma) \approx \sigma(\tau + \sigma/2), \quad \sigma(F) \approx \sqrt{2F + \tau^2} - \tau, \quad (\text{A15})$$

$$\varphi(F) \approx \frac{3}{2} [(2F + \tau^2)^{3/2} - \tau(3F + \tau^2)]$$

$$F_\xi \approx \left[F_0^{1/4} - \lambda_1 \xi + \frac{3\tau}{2^{5/4}(F_0^{1/4} - \lambda_1 \xi)} \right]^4,$$

with $\lambda_1 = k/(2^{3/4}\sqrt{3})$, obtaining the charge density distribution (Fig. 11)

$$\sigma(\xi) \approx (\sqrt{\sigma_0 + \tau} - \lambda_1 \xi)^2 - \tau. \quad (\text{A16})$$

This function seems to become zero as soon as $\xi = (\sqrt{\sigma_0 + \tau} - \sqrt{\tau})/\lambda_1$, but in fact the fast parabolic decay by Eq. (A16) only extends to $\xi \sim \xi^*$ such that $\sigma_{\xi^*} \sim \rho_e$, and for $\xi > \xi^*$ the decay becomes exponential, like Eq. (29). The I - V characteristics, Eq. (32), follows directly from Eq. (A16).

¹P. Sheng and B. Abeles, *Phys. Rev. Lett.* **28**, 34 (1972).

²P. Sheng, B. Abeles, and Y. Aire, *Phys. Rev. Lett.* **31**, 44 (1973).

³A. E. Berkowitz, J. R. Mitchell, M. J. Carey, A. P. Young, S. Zhang, F. E. Spada, F. T. Parker, A. Hutten, and G. Thomas, *Phys. Rev. Lett.* **68**, 3745 (1992).

⁴L. F. Schelp, A. Fert, F. Fetta, P. Holody, S. F. Lee, J. L. Maurice, F. Petroff, and A. Vaurés, *Phys. Rev. B* **56**, R5747 (1997).

⁵J. Varalda, W. A. Ortiz, A. J. A. Oliveira, B. Vodungbo, Y.-L. Zheng, D. Demaille, M. Marangolo, and D. H. Mosca, *J. Appl. Phys.* **101**, 014318 (2007).

⁶M. A. Parker, K. R. Coffey, J. K. Howard, C. H. Tsang, R. E. Fontana, and T. L. Hylton, *IEEE Trans. Magn.* **32**, 142 (1996).

⁷I. S. Beloborodov, A. V. Lopatin, V. M. Vinokur, and K. B. Efetov, *Rev. Mod. Phys.* **79**, 469 (2007).

⁸V. I. Kozub, V. M. Kozhevnikov, D. A. Yavsin, and S. A. Gurevich, *JETP Lett.* **81**, 226 (2005).

⁹Tai-Kai Ng and Ho-Yin Cheung, *Phys. Rev. B* **70**, 172104 (2004).

¹⁰G. N. Kakazei, P. P. Freitas, S. Cardoso, A. M. L. Lopes, Yu. G. Pogorelov, J. A. M. Santos, and J. B. Sousa, *IEEE Trans. Mag.* **35**, 2895 (1999).

¹¹B. Dieny, S. Sankar, M. R. McCartney, D. J. Smith, P. Bayle-Guillemaud, and A. E. Berkowitz, *J. Magn. Magn. Mater.* **185**, 283 (1998).

¹²G. N. Kakazei, A. M. L. Lopes, Yu. G. Pogorelov, J. A. M. Santos, J. B. Sousa, P. P. Freitas, S. Cardoso, and E. Snoeck, *J. Appl. Phys.* **87**, 6328 (2000).

¹³D. M. Schaadt, E. T. Yu, S. Sankar, and A. E. Berkowitz, *Appl. Phys. Lett.* **74**, 472 (1999).

¹⁴N. F. Mott and E. A. Davis, *Electronic Processes in Non-crystalline Materials* (Clarendon, Oxford, 1979).

¹⁵H. G. Silva, H. L. Gomes, Y. G. Pogorelov, L. M. C. Pereira, G. N. Kakazei, J. B. Sousa, J. P. Araújo, J. F. L. Mariano, S. Cardoso, and P. P. Freitas, *J. Appl. Phys.* **106**, 113910 (2009).

¹⁶I. O. Kulik and R. I. Shekhter, *Zh. Eksp. Teor. Fiz.* **68**, 623 (1975) [*Sov. Phys. JETP* **41**, 308 (1975)].

¹⁷J. A. M. Santos, G. N. Kakazei, J. B. Sousa, S. Cardoso, P. P. Freitas, Yu. G. Pogorelov, and E. Snoeck, *J. Magn. Magn. Mater.* **485**, 242 (2002).

¹⁸H. Silva, H. L. Gomes, Yu. G. Pogorelov, P. Stallinga, D. M. de Leeuw, J. P. Araújo, J. B. Sousa, S. C. Meskers, G. Kakazei, S. Cardoso, and P. P. Freitas, *Appl. Phys. Lett.* **94**, 202107 (2009).